

NACA RM L53D15a

TECH LIBRARY KAFB, NM
0144406

NACA

RESEARCH MEMORANDUM

LOAD DISTRIBUTIONS ASSOCIATED WITH CONTROLS AT
SUPERSONIC SPEEDS

By K. R. Czarnecki and Douglas R. Lord

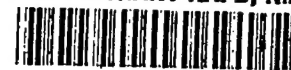
Langley Aeronautical Laboratory
Langley Field, Va.


NATIONAL ADVISORY COMMITTEE
FOR AERONAUTICS

WASHINGTON

May 29, 1953

317.98/13



0144406

1W

NACA RM L53D15a

~~CONFIDENTIAL~~

NATIONAL ADVISORY COMMITTEE FOR AERONAUTICS

RESEARCH MEMORANDUM

LOAD DISTRIBUTIONS ASSOCIATED WITH CONTROLS AT
SUPERSONIC SPEEDS

By K. R. Czarnecki and Douglas R. Lord

SUMMARY

The status of the control loads problem at supersonic speeds at the present time is discussed briefly, and some recent test results concerning the aerodynamic loads associated with various types of controls at supersonic speeds are presented. Analysis of the results indicates that, for three-dimensional wings having tip- or flap-type controls at large angles of attack and control deflections, it is necessary to consider the viscous effects, such as separation ahead of the deflected flap-type control, unporting at the wing-control parting lines, separation of the flow from the wing or control low-pressure surface, and the limiting pressures, in any attempt to predict the experimental loadings. On two-dimensional balanced trailing-edge control applications, the wing and control loadings can be predicted with reasonable accuracy except for the balancing portion of the control, so long as the unporting effect of the control leading edge on the wing loading is small. The loads associated with two-dimensional spoilers can also be calculated and the calculations may be applied to three-dimensional installations of spoilers provided that the spoiler is not operating in a region of flow which is separated from the wing leading edge.

INTRODUCTION

Until recently few experimental data have been available on the loads associated with various controls at supersonic speeds. In order to establish the limitations of existing theoretical methods and to develop improved methods of estimating control loads, the Langley Aeronautical Laboratory of the National Advisory Committee for Aeronautics has undertaken a number of investigations of control loads at supersonic speeds. The types of controls investigated include tip and trailing-edge controls on three-dimensional wings, controls with overhang balance on a two-dimensional wing, and spoiler controls on both two- and three-dimensional wings. Pressure-distribution and hinge-moment measurements were made in these investigations.

~~CONFIDENTIAL~~~~Hasen~~

This paper discusses briefly the present status of the control loads problem at supersonic speeds and presents some typical results from the more recent control loading investigations. The experimental results are compared with linear theory and with improved methods of analysis where such methods have been developed. In particular, emphasis is placed on conditions where the usual linear theory becomes inadequate.

SYMBOLS

M	stream Mach number
R	Reynolds number based on wing mean aerodynamic chord
q	stream dynamic pressure
p	stream static pressure
p_l	local surface pressure
P	pressure coefficient, $\frac{p_l - p}{q}$
P_R	resultant pressure coefficient, Lower-surface P - Upper-surface P
P_{Rc}	average section pressure-coefficient differential across spoiler
c_n	section normal-force coefficient
$c_n \frac{c}{\bar{c}}$	span-loading coefficient
c	wing local chord
\bar{c}	wing average chord
A	wing aspect ratio (based on wing with right and left panels)
Λ	wing leading-edge sweep angle
λ	wing taper ratio
α	wing angle of attack
δ	control deflection relative to wing

CONTROL CONFIGURATIONS INVESTIGATED

The first two figures (figs. 1 and 2) show a brief résumé of the scope of the loads investigations being made. On the left side of figure 1 is shown the trapezoidal wing which has been tested in the Langley 4- by 4-foot supersonic pressure tunnel at Mach numbers of 1.6 and 2.0 for a Reynolds number range from 1.6×10^6 to 6.5×10^6 . This wing has a modified hexagonal section of 4.5-percent thickness with sharp leading and trailing edges and a flat midsection. Six flap-type control configurations have been tested on the wing in order to determine the effect of control plan form, position, and trailing-edge thickness on the control loadings. Tests were made for angles of attack from 0° to 15° for control deflections from -30° to 30° . A typical group of orifice stations is shown.

On the right side of the same figure, the two-dimensional balanced trailing-edge controls (ref. 1) which have been tested in the Langley 9-inch supersonic tunnel are shown. The wing was 6 percent thick and the investigation was made at a Mach number of 2.4 and a Reynolds number of 0.8×10^6 , with and without fixed transition. Tests were made for angles of attack from 0° to 10° for control deflections from -20° to 20° . The variables considered were: gap between the wing and control, amount of balance of the control, control profile, and wing trailing-edge bevel.

In figure 2 is shown the delta wing which has been tested in the Langley 4- by 4-foot supersonic pressure tunnel for approximately the same range of conditions as has the trapezoidal wing. This wing was 3 percent thick at the root with a round leading edge, flat midsection, and tapered trailing edge. Eleven control configurations were tested with this wing, seven of the tip-type and four of the more conventional flap-type. Variations in the flap controls amounted to changing the trailing-edge thickness and testing the inboard and outboard sections of the full-span control, together and independently.

In addition to the controls shown in these two figures, detailed two-dimensional studies have been made of the flow over a spoiler at $M = 1.93$ in the Langley 9-inch supersonic tunnel (ref. 2), and an extensive investigation of the effect of attaching a spoiler to three-dimensional wings has been made in the Langley 4- by 4-foot supersonic pressure tunnel at $M = 1.6$ and 2.0.

DISCUSSION OF RESULTS

Before the control loadings determined in these investigations are discussed, note that it has been established previously that, at supersonic speeds, the chordwise loadings on flap-type controls were essentially rectangular in nature and that the spanwise loadings were fairly uniform for regions not strongly influenced by end effects. Further, investigations in the Langley 9-inch supersonic tunnel (refs. 3 and 4) and in the Langley 9- by 9-inch Mach number 4 blowdown jet (ref. 5) indicated that for controls in essentially two-dimensional flow, shock-expansion theory was in excellent agreement with experimental results when the boundary layer was turbulent. For the purposes of this paper, these findings are presumed to apply to the appropriate regions and the main part of the paper illustrates and discusses conditions where these findings do not apply. More specifically, the main discussion is limited to illustrations of the loadings associated with one of the flap and one of the tip controls on the delta wing, the full-span flap control on the trapezoidal wing, a few of the two-dimensional overhang-balanced controls, and some two- and three-dimensional applications of spoilers.

Loads on a Trailing-Edge Control on a Delta Wing

In figure 3 is shown a typical spanwise variation of the chordwise loadings on the delta wing equipped with the full-span trailing-edge control for a moderate angle of attack, 6° , and a large control deflection, 30° . The Mach number is 1.6. The figure illustrates two important effects which will be discussed in more detail in connection with subsequent figures. One of these effects is the large amount of load carryover ahead of the hinge line due to separation of the turbulent boundary layer ahead of the lower or high-pressure surface of the control as a result of shock-boundary-layer interaction. The other effect is the increase in loading experienced by the control along the span toward the wing tip. This increased tip loading occurs as a consequence of the conical flow over a delta wing at angle of attack which induces the highest wing loadings along the wing leading edge when the leading edge is subsonic. The high experimental loadings shown along the wing leading edge in this figure are evidences of this conical flow.

Typical experimental and theoretical loadings due to control deflection alone are shown in figure 4 for three stations on the control configuration shown in figure 3. The pressure loading is plotted against percent root chord; therefore, the leading-edge locations for the local chords are shown by ticks. Inasmuch as the wing is at zero angle of attack, the linear theory predicts that the entire load will be carried

on the control and that the distribution will be rectangular except when the Mach line from the intersection of the wing leading edge and the control hinge line crosses the orifice station. At this control deflection of 20° , the experimental load is beginning to build up ahead of the control because of the turbulent boundary separation. It was found that, for the Mach numbers of these tests, the turning angle of the control lower surface which causes the initial separation was always near 13° , except when the local Mach number was less than 1.4.

The experimental loading on the control is essentially rectangular; however, the linear theory generally overestimates the loading by a significant amount. By neglecting the thickness effect, assuming linear theory for the lifting pressures to be adequate ahead of the hinge line, and using two-dimensional shock-expansion theory to predict the control loading, the agreement between theory and experiment is improved. Flow studies also show that, at these large deflections, the trailing-edge shock causes separation from the control upper surface, and here again the separation angle is approximately 13° . If this separation from the control upper surface is considered, good agreement between theory and experiment is obtained. At station 6, the agreement is poorer than at the inboard stations because of the tip effect. Beyond the point where separation occurs on the lower wing surface ahead of the hinge line, or beyond 20° deflection for this particular control, the exact procedure for applying the combined linear-theory—shock-expansion—separation technique for estimating loads has as yet not been established because of the complicated way in which the separated flow reattaches to the control ahead of the trailing edge.

The experimental and theoretical combined loadings due to an angle of attack of 12° and a control deflection of 20° are shown in figure 5. Leading-edge flow separation on the upper surface is known to exist for this condition. The separation limit line shown on the sketch of the wing plan form was determined from the upper-surface pressure distributions and indicates the extent of the separated region from the leading edge.

The carryover of load ahead of the hinge line has increased slightly because of the addition of angle of attack to the condition shown on the previous figure (fig. 4). At station 6, the flow is completely separated and the experimental loading bears little resemblance to the linear-theory prediction. The linear-theory predictions of control loadings are again much too large; however, by using the shock-expansion technique previously described and considering the separation from the control upper surface, it is possible to get a much closer approximation to the experimental loadings. Hence, it may be concluded that by the judicious use of the combined linear-theory—shock-expansion—separation theory, control loadings can be estimated with good accuracy for this type of control except when the flow begins to separate ahead of the hinge line and except in regions affected by tip effects or leading-edge separation.

In figure 6 are shown spanwise loadings and center-of-pressure locations for the full-span trailing-edge control on the delta wing for conditions which cannot be handled by the advanced theoretical technique. Curves are shown for the load on the control alone and for the complete wing. The angle of attack is only 6° , but the control deflection is 30° . The results indicate that linear theory badly overestimates the control loading at all stations across the span and that it underestimates the effect of angle of attack on the span load distribution. The shape of the predicted and experimental spanwise loadings for the complete wing are in good agreement, and, although the linear theory overestimates the loads, the discrepancy between theory and experiment is much less than for the control alone. Since it would be expected that the deficiency in control loading would also be evident on the complete wing loading, the improvement in agreement must be due to the increased load on the wing from the carryover.

The linear-theory prediction of the spanwise variation of the chordwise center of pressure of the load on the control, shown on the right of the figure, is in good agreement with the experimental results. The linear theory predicts a somewhat more rearward location of the center of pressure for the complete wing than is obtained experimentally because of the aforementioned forward carryover of the control load.

Loads on a Tip Control on a Delta Wing

A typical spanwise variation of the chordwise loadings on the delta wing having a tip control is shown in figure 7. The wing is at an angle of attack of 6° and the control deflection is 30° , although, for purposes of clarity, the control is shown undeflected. Along the wing leading edge, the rounded distribution characteristic of leading-edge separation is again evident. Farther back along the wing stations, violent loading changes occur because of the unporting effect between the wing and control at the parting line which allows an interchange of pressure from the high-pressure side of the control to the low-pressure side of the wing and from the high-pressure side of the wing to the low-pressure side of the control. These abrupt loading variations occur on both the wing and control and are more pronounced at the stations immediately adjacent to the parting line and tend to fade out with distance from this line.

In figure 8 are shown typical experimental and linear-theory loadings on the tip-control configuration due to control deflection only. Loadings are shown for three typical stations at 20° deflection. In the present case, the linear theory predicts that some load will be carried on the wing behind the Mach line from the control apex. At the inboard wing station, linear theory and experiment are in fair agreement, the load being carried on only the last 20 percent of the chord. Near

the parting line, the experimental variation of loading is erratic, and neither the shape nor magnitude of the loading is predicted by linear theory. As previously noted, this effect might be expected since the linear theory does not take into account any unporting of the control. On the control itself, the upper-surface flow tends to separate from the leading edge, with the extent of the separation increasing from the control apex outboard as shown by the separation limit line on the plan-form view. At station 6, therefore, the flow is separated over much of the upper surface and the experimental loading does not agree with the theoretical loading. The sudden loss in loading at this station behind the 90-percent root-chord station is due to the separation of the flow from the control upper surface previously noted which precludes the expansion around the corner present on the upper surface at that station. It should be mentioned at this point that at the present time no improved theoretical methods of estimating detailed loadings comparable to that of the trailing-edge control are available for the tip-control configuration.

In figure 9 are shown the experimental and theoretical combined loadings due to an angle of attack of 12° and a control deflection of 20° for the same delta wing and tip control. For this condition, the leading-edge separation starts from the wing apex and covers a large share of the wing and most of the control. At the inboard station, the experimental and theoretical loadings due to angle of attack agree fairly well, but the experimental results indicate little effect due to control deflection. Near the parting line, the agreement over part of the chord is good; however, this agreement is fortuitous in view of the erratic behavior of the loads in this region which cause changes such as that near the trailing edge at this station. At station 6 on the control, the upper-surface flow is completely separated and the linear theory completely overestimates the loading. This overestimation of load is to be expected, inasmuch as at these high angles of inclination of the surface to the air flow, the pressures on the lower surface approach a positive limit (stagnation pressure) and the pressures on the upper surface approach absolute vacuum; therefore, the linear theory which permits the addition of the pressures due to angle of attack and the pressures due to control deflection is no longer valid. Obviously, for this type of control, considerably more analysis is required before satisfactory methods of estimating detailed loadings can be developed.

In figure 10 are shown the experimental and theoretical spanwise loadings and center-of-pressure locations for the tip control on the delta wing. The curves are presented for an angle of attack of 6° with control deflections of 0° and 30° . With the control undeflected, the linear-theory prediction of the loading is in excellent agreement with the experiment, except near the tip where there is a small loss in experimental lift. When the control is deflected, the experimental control loading is considerably less than the theoretical control loading and the spanwise variation of the loading is considerably more linear. In addition, there is little or no carryover load on the wing. This lack of experimental load carryover occurs for nearly all angles of attack and control deflection.

The linear-theory prediction of the center of pressure of the loads on the wing and control are in good agreement, both for the undeflected and the deflected control, despite the differences in loadings shown. On the basis of these experimental results and similar spanwise loadings and center-of-pressure locations at other angular conditions and for other tip-control configurations, it is possible to make fairly reasonable estimates of over-all control bending and hinge moments for tip-type controls despite the inadequacy of the linear theory.

Application of Results to Other Delta-Wing Control Configurations

Returning to figure 2, an examination of the various control configurations tested shows that the general conclusions concerning the loads associated with the tip control and flap control already discussed will apply to the other related controls. Ahead of the trailing-edge controls the turbulent boundary layer separates when the deflected control causes a sufficiently large pressure rise. At high control deflections, the separation of the flow from the low-pressure surface and the limiting pressures must be taken into account in any attempt to predict the loadings. Near chordwise parting lines, loadings will be erratic and carryovers negligible. The effect of trailing-edge bevel is to change the angles of control deflection at which separation at the hinge line and on the suction surface will appear. The 13° criterion will still hold.

Comparison of Control Loadings on a Delta and a Trapezoidal Wing

A comparison of the spanwise loadings of trailing-edge controls on a delta and a trapezoidal wing is presented in figure 11. The angle of attack is 6° ; the control deflection is 30° . The test Mach number is 1.6. In general, the loadings on the controls on both wings are similar if allowance is made for the taper on the trapezoidal-wing control. On the delta-wing control, however, an increase in angle of attack tends to increase the loading on the outboard hinges. No such change in load distribution occurs on the control on the trapezoidal wing with increasing angle of attack except for a very small region close to the wing tip where the tip vortex begins to form. Obviously, the method previously presented for estimating detailed loadings on the delta-wing control will apply even more readily to estimations of loads on the trapezoidal wing for control deflections below the critical value. For control deflection above the critical value the only available theory (linear theory) is, of course, inadequate as indicated by figure 11.

Loadings on Two-Dimensional Controls With Overhang Balance

Some of the more important loading characteristics found in tests of two-dimensional flap-type controls with overhang balance are shown in the next three figures. In figure 12 is shown a comparison of the pressure distributions and schematic diagrams of the flow over a typical control configuration with and without bevel of the wing ahead of the control. The angle of attack is 8° , the control deflection is 8° , and the test Reynolds number is 0.8×10^6 for a Mach number of 2.41. Transition was fixed in order to assure a turbulent layer.

On the blunt trailing-edge wing, the flow follows the airfoil contours to the wing trailing edge as indicated in the upper left sketch in figure 12. Behind the trailing edge the wake is very wide and the balance or forward part of the control is immersed largely in a dead-air region. Behind the hinge line the flow generally follows the contour of the control. The experimental pressure distribution corresponding to this flow is shown as a solid line in the plot at the lower left. The theoretical pressure distribution, obtained by means of shock-expansion theory, is shown as dashed lines. Because of the complicated nature of the flow, no theoretical pressures were computed over the control ahead of the hinge line; behind the hinge line, the pressures were computed as if this part of the control were attached directly to the main wing, without forward balance, without any dead-air region, and without any surface discontinuity. A comparison of the theoretical and experimental results shows remarkably good agreement for those parts of the wing and control for which theoretical calculations were made, despite the neglect of the balancing portion of the control. The experimental load on the control balance is negligible, as is to be expected, except where the flow from the lower wing surface impinges slightly ahead of the hinge line.

On the beveled trailing-edge wing the flow does not follow the airfoil contour completely but separates from the upper wing surface ahead of the trailing edge as indicated in the upper right diagram in figure 12. This separation of the turbulent boundary layer occurs as a result of the unporting of the control leading edge. In this respect, the projecting nose of the control acts in the same manner as a spoiler. On the lower surface of the wing the flow impinges much closer to the control leading edge than for the case of the blunt wing. The corresponding theoretical and experimental pressure distributions are indicated in the plot at the lower right. On the upper wing surface behind the fifty-percent-chord station, the separated flow causes an increase in pressure, hence, a decrease in wing loading. On the balance, the pressures on the lower surface are higher and cover a wider area. Except for the separated region, theoretical and experimental pressures are again in good agreement.

In figure 13 is shown the effect of fixing transition on the chord-wise loading for a typical control configuration on the blunt trailing-edge wing. The shock-expansion theory predicts the loading very well in the turbulent case, both on the wing and on the control behind the hinge line. In the laminar flow case, the loading over the rear of the wing and over the control behind the hinge line does not agree as well with the shock-expansion theory because of the separation of the laminar boundary layer from the upper surface of the wing and control. Laminar boundary layers are very susceptible to separation at supersonic speeds. In the simpler cases, laminar separation can be treated in a manner similar to that proposed earlier for the turbulent boundary layer, except that the flow separation angles are on the order of 1° to 3° rather than approximately 13° .

The effect of control unporting on the blunt wing is illustrated in figure 14. The results are shown for the control with 82-percent balance with laminar boundary layer. At 8° control deflection the control is unported and has no effect on the loading over the wing. The control leading edge operates in a dead-air region; therefore, the balance loading is negligible. The experimental results are in good agreement with theory except behind the hinge line where laminar separation occurs on the upper control surface.

When the control is deflected to 20° , the leading edge unports and the flow on the upper wing surface is separated. Because the boundary layer is laminar, separation occurs as far forward as the corner at the 30-percent station. If it is assumed that the lower surface of the control balance is in a dead-air region and that the upper-surface flow attaches to the control at the leading edge and, hence, follows the control contours, then the theoretical loadings indicated herein are obtained. The experimental and theoretical loadings on the balance are in fair agreement, but the loadings on the control behind the hinge line are not. This discrepancy occurs because a small amount of flow from the upper surface through the gap tends to deflect the lower-surface flow downward so that it impinges on the control near the trailing edge.

In considering the remaining variables of the tests, mentioned in the discussion of figure 1, it may be stated that the effect of increasing the gap between the wing and control was to make the control behave more like an isolated airfoil. The effect of increasing the balance was to reduce and spread out the peak load ahead of the hinge line because of the reduction in leading-edge angle of the control. Making the control nose elliptical made the unporting effects appear at lower control deflections. Blunting the trailing edge simply changed the control angles for trailing-edge separation as discussed previously for the flap control on the delta wing.

Loads Due to Spoilers

In order to gain a little insight into some of the characteristics of spoiler loadings at supersonic speeds a two-dimensional schlieren photograph, a schematic flow diagram, and a pressure distribution are shown in figure 15. These tests were made at a Mach number of 1.93 for a Reynolds number of 1.87×10^6 , and the condition presented is for an angle of attack of 0° with a 5-percent-chord height spoiler at the 70-percent-chord station. The flow over the surface may be traced by the arrows through the leading-edge shock, past the transition fix, then through the expansion around the corner. Some distance ahead of the spoiler the flow separates, causing a shock at the separation point and a dead-air region ahead of the spoiler. The flow then expands around the spoiler and tends to follow the rear surface of the spoiler. Because of the presence of the wing, however, the flow separates and reattaches to the wing some distance behind the spoiler. In this reattachment process the flow is usually turned through two angles as indicated by the double shock.

Without the spoiler, the shock-expansion theory (dashed line) adequately estimates the pressure variation along the wing. When the spoiler is attached, the method of Donaldson and Lange (ref. 6) may be used to predict the separation point and pressure rise ahead of the spoiler as shown by the dotted line. The remaining part of the flow was calculated by a rather lengthy iteration procedure based on the flow diagram just discussed. Indications are, nevertheless, that the calculations may be reduced to a simpler flow model involving an initial separation angle of about 13° and an empirically determined ratio of spoiler expansion angle to initial separation angle.

In order to illustrate what might be a limiting case of the applicability of two-dimensional spoiler results to a three-dimensional wing, the results of tests of an unswept spoiler mounted on a delta wing are shown in figure 16. The spoiler height was 5 percent of the wing mean aerodynamic chord and the tests were made at a Mach number of 1.6 for a Reynolds number of 4.2×10^6 . Pressure distributions for two stations on the wing are shown in figure 16 for an angle of attack of 12° with the spoilers mounted on the upper or lower surface and with no spoiler on the wing. The calculated separation pressures are based on linear-theory lifting pressures for the wing, neglect of thickness effects, and the assumption of a separation angle of 13° . At the inboard station the effect of the spoiler on the pressure distributions was very similar to that previously shown for the two-dimensional tests. There is a sharp pressure rise ahead of the spoiler, an essentially constant pressure to the spoiler, and then a large expansion and subsequent compression to the trailing edge. At the outboard station, the lower-surface-spoiler effect is still the same; however, the pressure rise ahead of the

upper-surface spoiler is almost eliminated. It appears that, since the flow towards the tip of a delta wing tends to separate fairly easily at high angles of attack, in this case the spoiler has caused upper-surface separation from the leading edge with the resultant change in characteristics.

The spanwise variation of the pressure differential across the spoiler, or spoiler chord force, is shown in the lower right of figure 16. The variation is generally constant except at an angle of attack of 12° with a spoiler on the upper surface when there is a decided decrease in chord force at the outer portion of the spoiler span due to the leading-edge separation just described.

CONCLUDING REMARKS

In summary, it may be said that there is available a large amount of loads data at supersonic speeds to aid in the estimation of control loads on all types of controls. Also, rapid progress is being made in improving theoretical and empirical techniques of estimating detailed or over-all loadings. As was pointed out in the discussions, nevertheless, much work yet remains to be done before the over-all problem can be considered solved.

Langley Aeronautical Laboratory,
National Advisory Committee for Aeronautics,
Langley Field, Va.

REFERENCES

1. Mueller, James N., and Czarnecki, K. R.: Preliminary Data at a Mach Number of 2.40 of the Characteristics of Flap-Type Controls Equipped With Plain Overhang Balances. NACA RM L52F10, 1952.
2. Mueller, James N.: Investigation of Spoilers at a Mach Number of 1.93 To Determine the Effects of Height and Chordwise Location on the Section Aerodynamic Characteristics of a Two-Dimensional Wing. NACA RM L52L31, 1953.
3. Czarnecki, K. R., and Mueller, James N.: Investigation at Mach Number 1.62 of the Pressure Distribution Over a Rectangular Wing With Symmetrical Circular-Arc Section and 30-Percent-Chord Trailing-Edge Flap. NACA RM L9J05, 1950.
4. Czarnecki, K. R., and Mueller, James N.: Investigation at Supersonic Speeds of Some of the Factors Affecting the Flow Over a Rectangular Wing With Symmetrical Circular-Arc Section and 30-Percent-Chord Trailing-Edge Flap. NACA RM L50J18, 1951.
5. Ulmann, Edward F., and Lord, Douglas R.: An Investigation of Flow Characteristics at Mach Number 4.04 Over 6- and 9-Percent-Thick Symmetrical Circular-Arc Airfoils Having 30-Percent-Chord Trailing-Edge Flaps. NACA RM L51D30, 1951.
6. Donaldson, Coleman duP., and Lange, Roy H.: Study of the Pressure Rise Across Shock Waves Required To Separate Laminar and Turbulent Boundary Layers. NACA TN 2770, 1952.

~~CONFIDENTIAL~~

NACA RM L53D15a

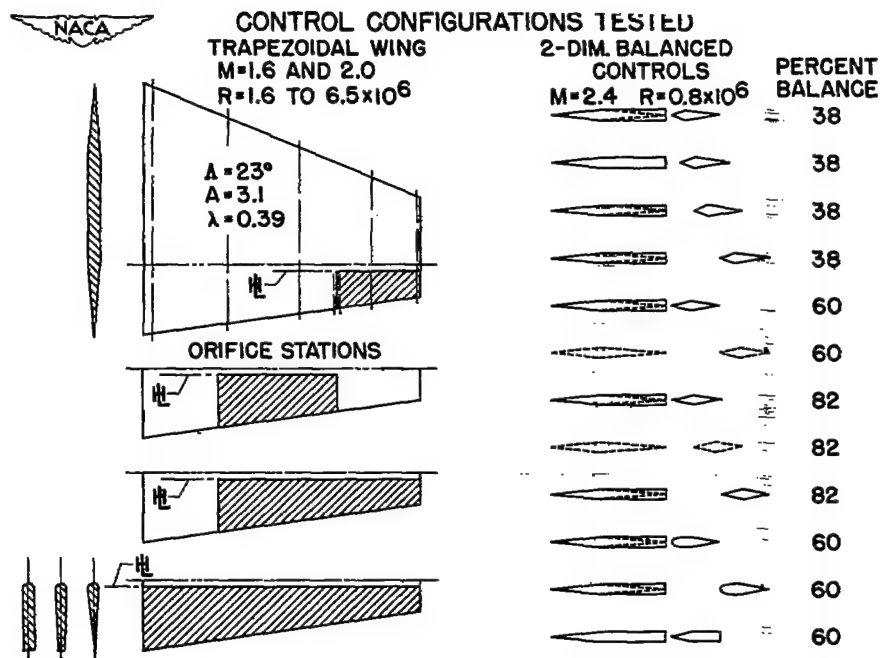


Figure 1.

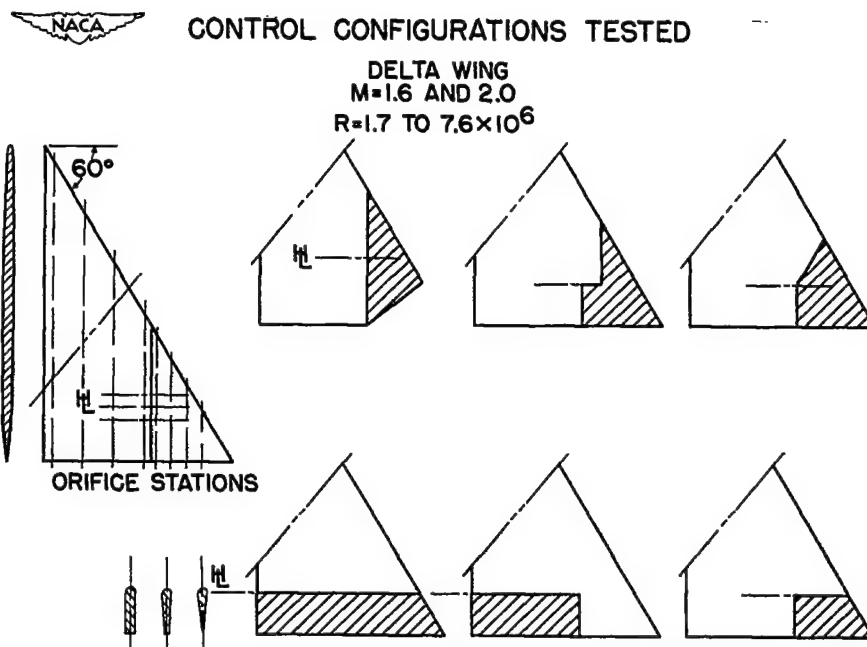


Figure 2.

~~CONFIDENTIAL~~

~~CONFIDENTIAL~~

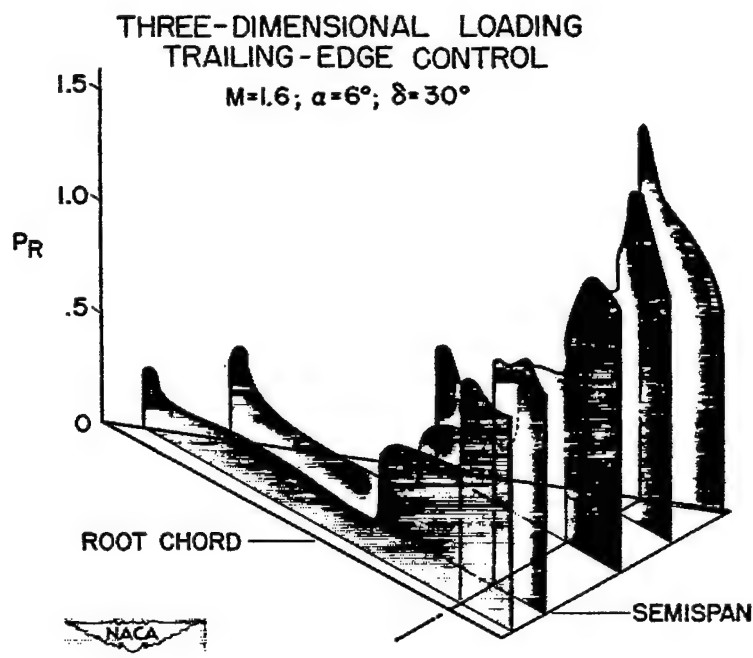


Figure 3.

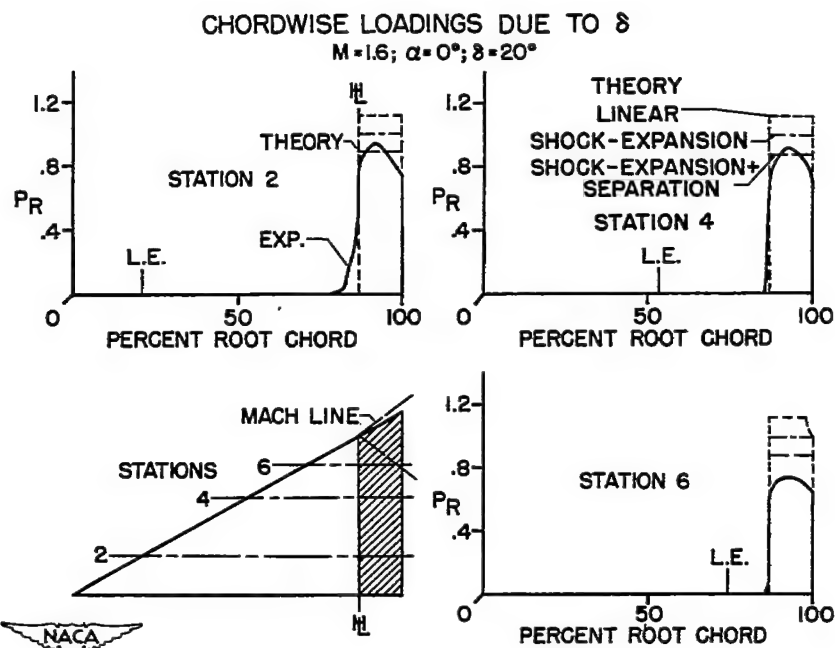


Figure 4.

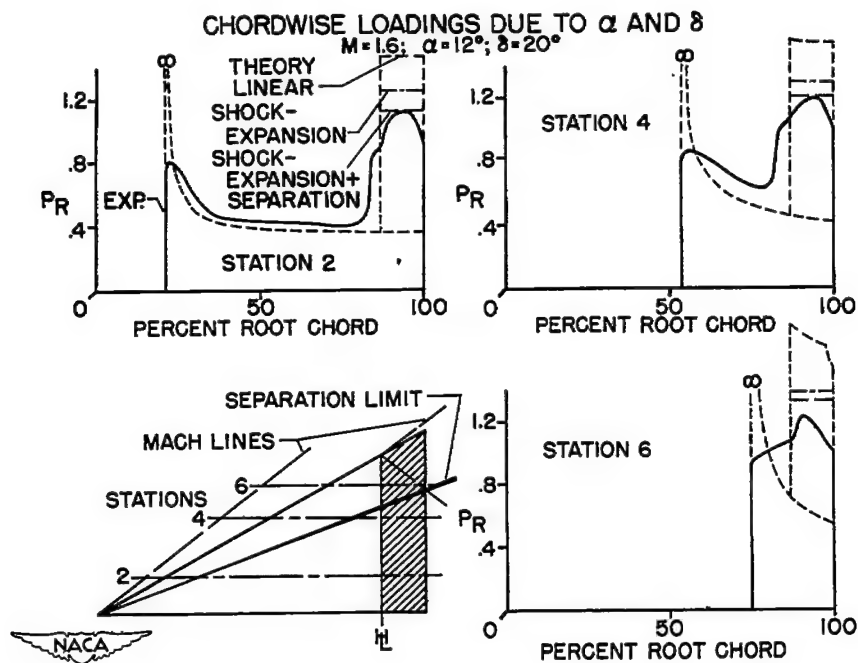


Figure 5.

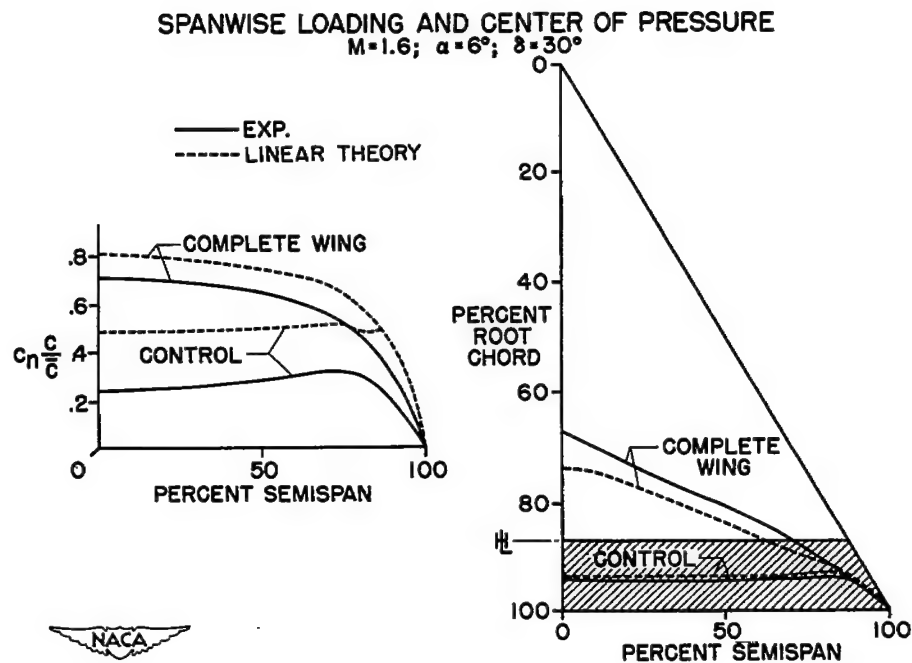


Figure 6.

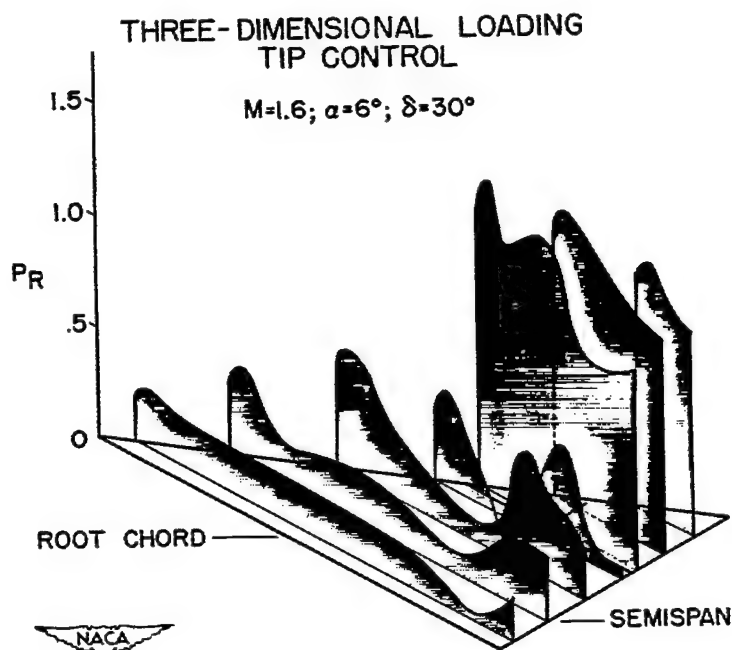


Figure 7.

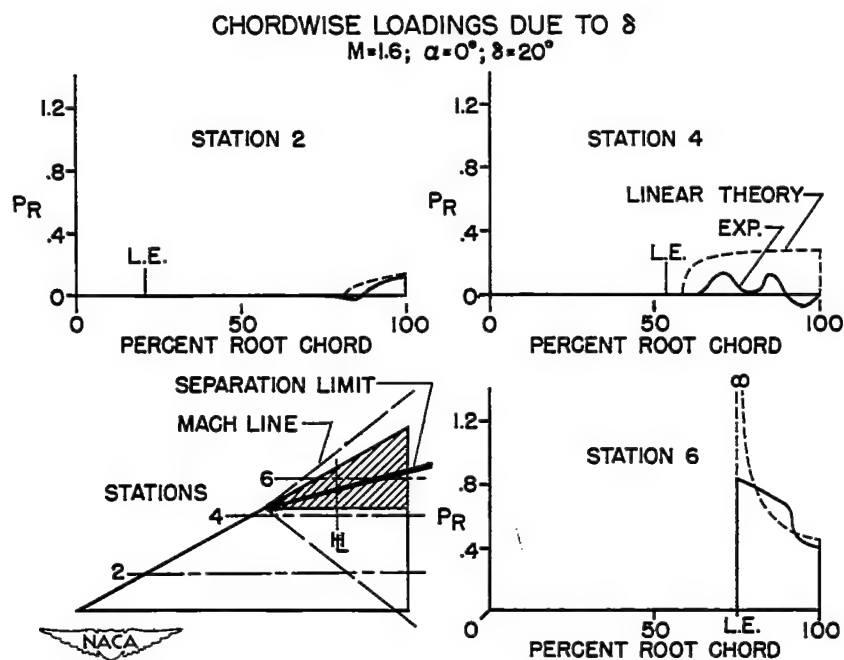


Figure 8.

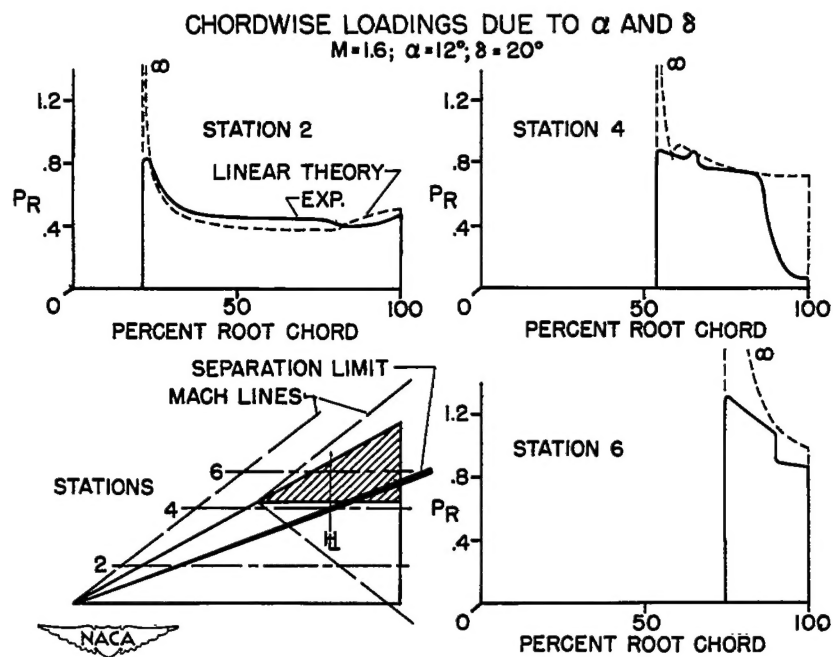


Figure 9.

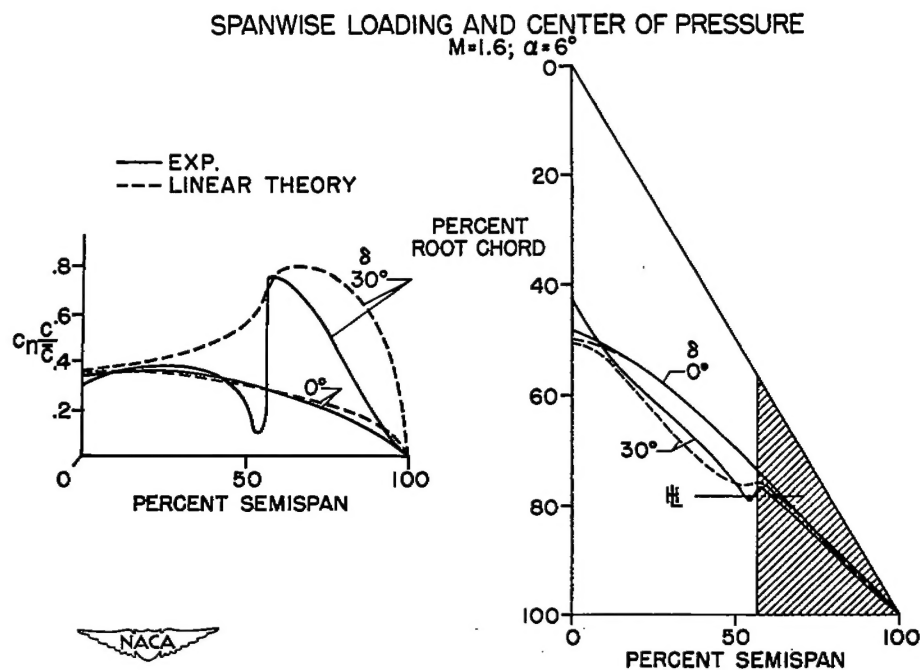
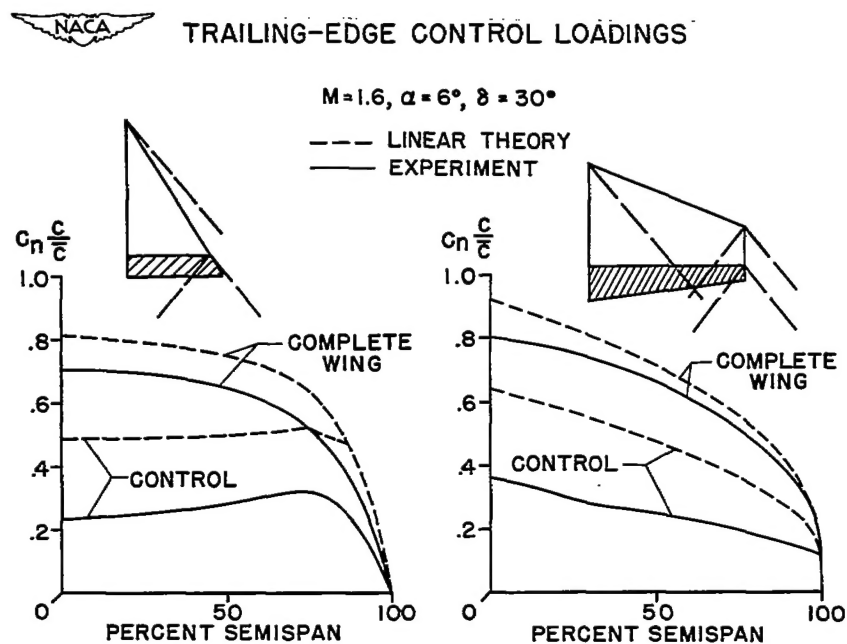
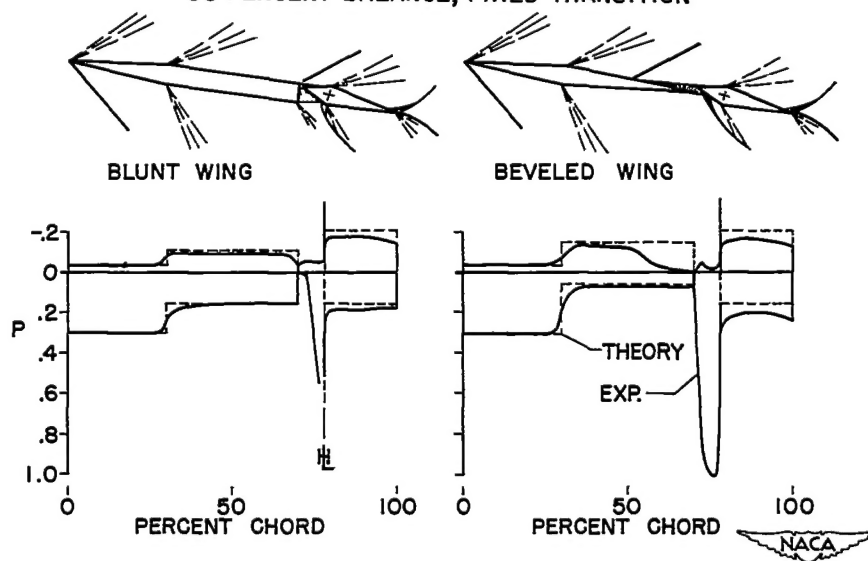


Figure 10.



FLOW CHARACTERISTICS—TWO-DIM. BALANCED CONTROL
 $M=2.41, R=0.8 \times 10^6, \alpha=8^\circ, \delta=8^\circ$
 38 PERCENT BALANCE, FIXED TRANSITION



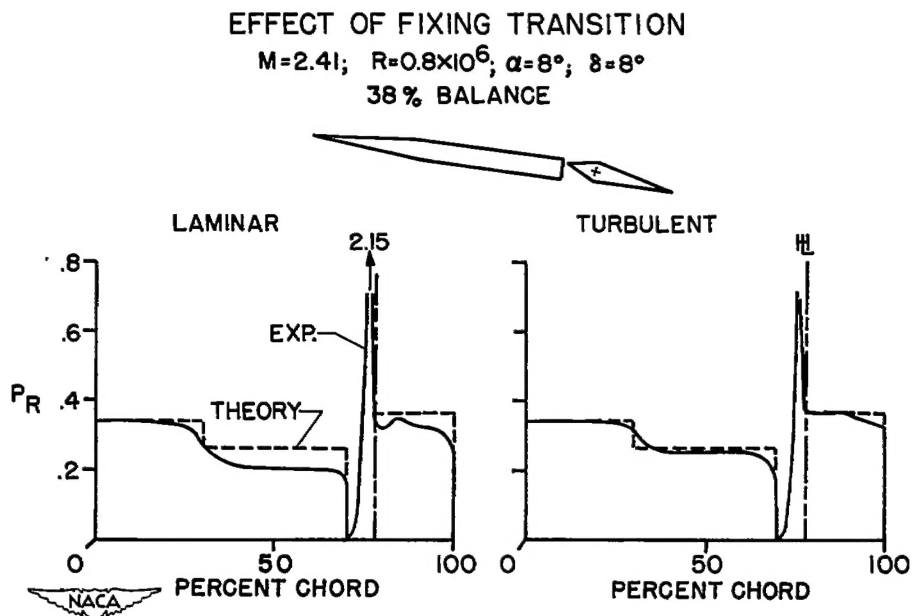


Figure 13.

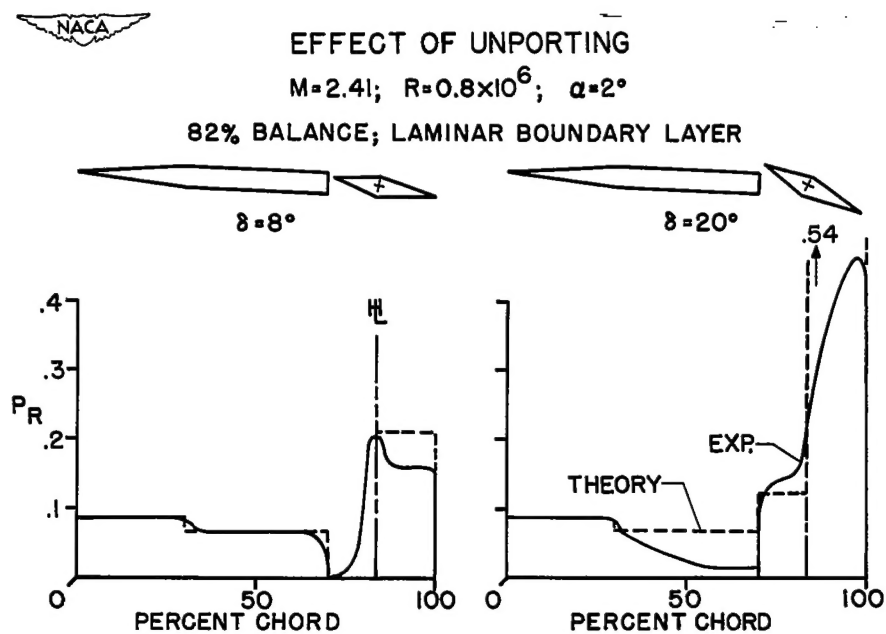


Figure 14.

TWO-DIMENSIONAL SPOILER FLOW

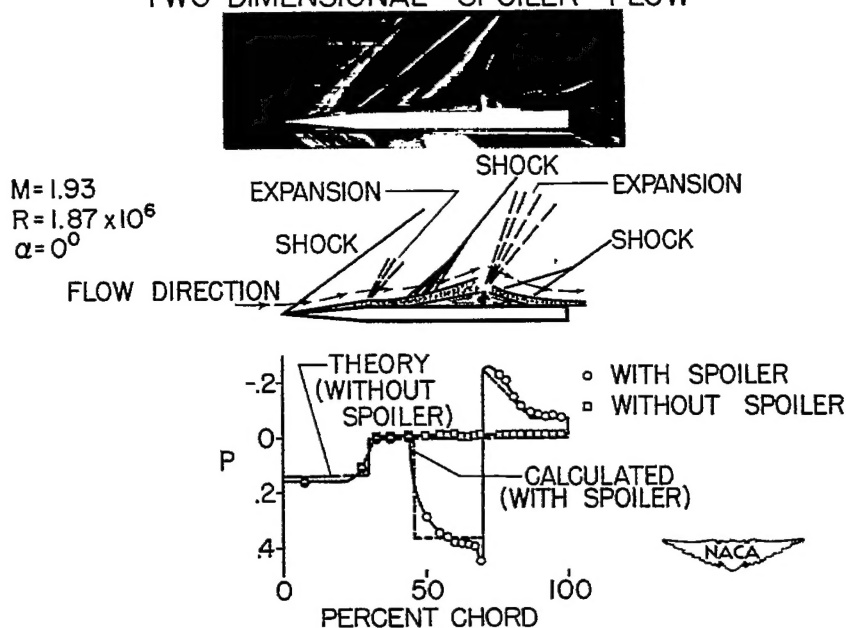


Figure 15.

THREE-DIMENSIONAL SPOILER CHARACTERISTICS

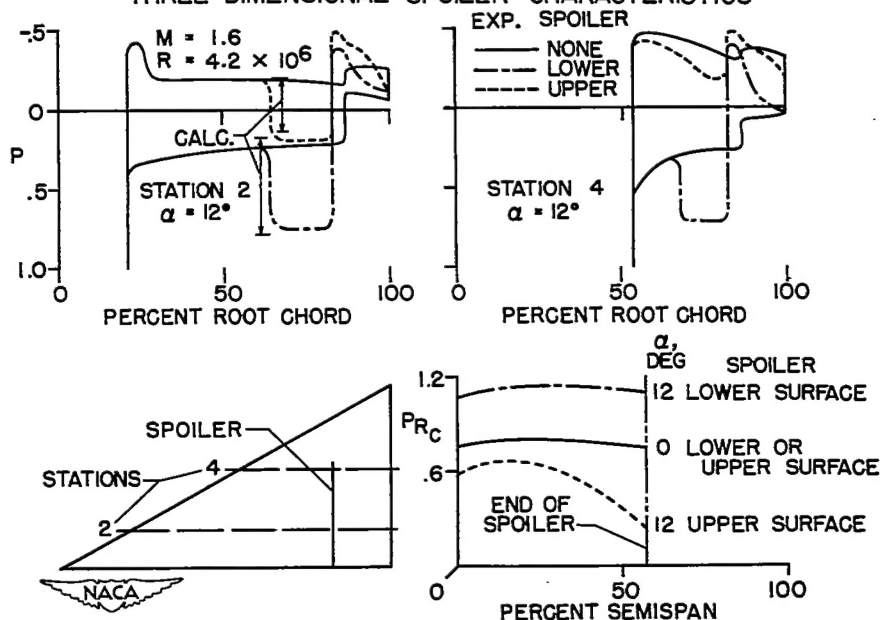


Figure 16.